Multisequential photofragmentation of size-selected gold cluster ions

M. Vogel
Institut für Physik, Johannes-Gutenberg-Universität, D-55099 Mainz, Germany

K. Hansen
Department of Physics, Post Box 35, FIN-40014 University of Jyväskylä, Finland

A. Herlert
Institut für Physik, Johannes-Gutenberg-Universität, D-55099 Mainz, Germany

L. Schweikhard
Institut für Physik, Ernst-Moritz-Arndt-Universität, D-17487 Greifswald, Germany

(Received 18 April 2002; revised manuscript received 21 June 2002; published 5 September 2002)

Time-resolved fragmentation measurements have been performed on stored, size-selected gold cluster ions Au_n^+ ($n=17-21$) that have been excited up to 15 eV by multiphoton absorption. These excitation energies are far above the clusters' dissociation thresholds and initiate multistep sequential unimolecular dissociation by evaporation of neutral monomers. The measurements allow for the determination of a combination of kinetic-energy release and radiative cooling of the excited clusters. Also, previously determined model-independent values of the cluster dissociation energies are confirmed by the present measurements. The data are consistent with thermal values of the kinetic-energy release with no significant radiative cooling of the excited clusters.

DOI: 10.1103/PhysRevA.66.033201 PACS number(s): 36.40.Qv, 36.40.Wa

I. INTRODUCTION

The dissociation energy is one of the fundamental properties of any polyatomic particle. It is closely related to the stability of the particle at finite temperatures. Whereas total binding energies can be found by calorimetric measurements for stable species which can be isolated in macroscopic amounts, the situation is more complicated for species that exist only in molecular beams. A particularly popular set of methods for the determination of binding energies of such molecules uses the unimolecular reaction theory, which presumably is so well established that precise dissociation energies can be extracted with confidence from energy-resolved measurements of rate constants [1–10]. Photofragmentation experiments are particularly close to the experiments here with respect to instrumentation. They differ in detail but are based on the measurement of a unimolecular rate constant, a decay probability, or a branching ratio. The experiments may be performed with known internal energy, as in the present case where the very precisely known energy of the photons can be added to the initial cluster excitation energy and the rate constant can be measured as a function of the total excitation energy. Alternatively, a broad and *a priori* unknown energy distribution can be used and the energy calibration can be provided by some process with a known activation energy. An elegant example of the latter is the use of the monomer-dimer branching ratio as the measured signal and the dimer binding energy as the energy calibration in the measurements of sodium cation stabilities [11]. However, the interpretation of these data requires that rate constants can be converted to energies or that ratios of rate constants in the form of measured branching ratios are converted to differences in binding energies. This requires an assumption about the transition state, or, in other words, the entropy of the emission channel. This is nontrivial as witnessed by the fact that the data in [11] were analyzed with the same rate constants for monomer and dimer emission, which is generally considered incorrect today. Also the caloric curves, or level densities, need to be known for the application of rate constant or branching ratio measurements. A number of formulas exist for calculating the vibrational spectra of clusters via some extrapolation from bulk properties. Combined with very efficient computer algorithms to calculate the absolute level density by direct counting or with analytical formulas for low-energy state counting, it seems that very powerful tools were available to calculate decay constants. This is, however, the case only till the excitation spectrum of the cluster can be represented by a collection of harmonic oscillators. At the fairly high energies where unimolecular reactions take place, the bulk values of the thermodynamic properties show a markedly nonharmonic tendency for a number of metallic elements. The simplest sign of this is the deviation of the heat capacity from the Dulong-Petit value of $3k_B$ per atom. On occasion Klots's finite heat bath theory [12] is used to provide supposedly model-free values of evaporative activation energies, but this theory includes the same assumptions concerning heat capacity, transition state, etc. as a direct calculation with a rate constant required.

Another set of methods which can be applied to wide ranges of cluster materials and sizes are based on fragmentation after collisions with either electrons or atoms. In the single-collision regime this technique provides an efficient way of transferring excitation energy to the cluster with a tunability and range which is not easily obtained with light sources. Measuring the amount of fragmented (or ionized) clusters or molecules in the beam as a function of the collision energy yields, by use of some modeling, the activation energy for the process. The modeling needed is contained in

an energy-transfer function which expresses how much energy is transferred to the cluster or molecule during the collision, and by the usual parametrization of the rate constant in terms of transition state and level densities of precursor and product cluster. In some cases this modeling can be avoided, namely, if the dissociation energies and caloric curves of two consecutive cluster sizes are identical. Then the rest energy in the cluster after the fragmentation, known as the kinetic shift, is the same for the two clusters, and the dissociation energy is just the difference in appearance energies of the two cluster sizes [13].

As mentioned, the caloric curve and the transition state are two potential sources of error in the calculation of the rate constants, which affect almost all of these methods. Also, radiative cooling can seriously distort the conclusions drawn from an uncritical application of unimolecular theory. The effects of radiation are at least twofold: It will decrease the fragment yield and will tend to increase the observed decay constant. The problem is emphasized by work on the radiative cooling of fullerenes, which has demonstrated that it is not possible to account for the radiative behavior from vibrational excitations alone [14].

Hence, detailed knowledge of a molecule is required for an accurate modeling of the decay. For a large number of clusters and molecules this information is not readily available and it is therefore desirable to have an alternative method to determine the dissociation energy that minimizes the number of assumptions involved in the analysis. Recently, such a method has been presented and applied to gold clusters Au_n^+ of sizes $n=14$–24 [15]. The method is based on the comparison of the dissociation process $B\rightarrow C$ with the sequential process $A\rightarrow B\rightarrow C$ and it yields the dissociation energy of the system A.

The method is model-free by nature but requires knowledge about the kinetic-energy release during the fragmentation $A\rightarrow B$ and about the amount of radiative cooling before A fragments. The effect of the uncertainty in these two energies on the resulting value of the dissociation energy is estimated to be small [15]. However, these numbers are experimentally accessible and in the following we describe and apply an extended version of the procedure, applied to Au_n^+ $(n=17$–$21)$, that not only allows an experimental test of the previously obtained model-free values, but also helps to determine a combination of the kinetic-energy release E_{KER} and the amount of radiative cooling during the first step of the multisequential dissociation.

II. METHOD

The method applied in this work is based on three-step multisequential dissociation processes $A\rightarrow B\rightarrow C\rightarrow D$. These are compared to sequential processes $B\rightarrow C\rightarrow D$. In both decay chains the last step, $C\rightarrow D$, occurs delayed and the rate constant of the last decay of a given chain serves as an uncalibrated thermometer for the energy content of B.

The multisequential dissociation has the form

$$Au_n^+ \rightarrow Au_{n-1}^+ \rightarrow Au_{n-2}^+ \overset{k}{\rightarrow} Au_{n-3}^+ \tag{1}$$

and is initiated by a photoexcitation energy $E_{ph}(n,n-3)$. The corresponding sequential dissociation starts one cluster size below and with the photoexcitation energy $E_{ph}(n-1,n-3)$:

$$Au_{n-1}^+ \rightarrow Au_{n-2}^+ \overset{k}{\rightarrow} Au_{n-3}^+ . \tag{2}$$

When the rate constants for the final steps are identical and in the absence of radiation, the dissociation energy of Au_n^+ is obtained as

$$D_n = E_{ph}(n,n-3) - E_{ph}(n-1,n-3) + (E_{th,n} - E_{th,n-1}) - E_{KER,n}(n,n-3), \tag{3}$$

where $E_{KER,n}(n,n-3)$ is the kinetic-energy release of the decay from n to $n-1$ in the decay chain $n\rightarrow n-3$. The two energies $E_{th,n}$ and $E_{th,n-1}$ are the room-temperature thermal energies acquired prior to the photoexcitation.

The contribution from the thermal energy has only a minute influence on the numerical determination of D_n. When the value used in [15] is adopted for the room-temperature thermal energy, the difference in thermal energies of the precursors in the multisequential and the sequential processes is $E_{th,n}-E_{th,n-1}=0.063(3)$ eV, where the uncertainty given is an estimate of the systematic error.

The kinetic-energy release can be measured directly, either by the recoil it imparts on the product cluster or by the kinetic-energy distribution of the evaporated atom [16–21]. The data presented here do not provide such a determination independently of the amount of radiative cooling and therefore a calculated estimate is compared with the data. With the same set of theoretical expressions as used in [15] the numbers are typically 0.3 eV for the first step in multisequential decays, with estimated systematic uncertainties, which are more than two orders of magnitude smaller than the typical shift in photoexcitation energy, $E_{ph}(n,n-3) - E_{ph}(n-1,n-3)$. They vary with the excitation energy but the absolute variation is small and an average value is therefore used.

Some rate constants for the direct decay and the last step of the sequential decay chains have been determined earlier [15]. They have been supplemented by further measurements (Fig. 3, see below). Specifically, those are the sequential decays terminating one cluster size higher,

$$Au_n^+ \rightarrow Au_{n-1}^+ \overset{k}{\rightarrow} Au_{n-2}^+ , \tag{4}$$

and the direct decay starting one size lower and terminating one size higher,

$$Au_{n-1}^+ \overset{k}{\rightarrow} Au^+_{n-2}, \tag{5}$$

which are initiated by photoexcitation energies $E_{ph}(n,n-2)$ and $E_{ph}(n-1,n-2)$, respectively.

The shifts in photoexcitation energy for the multisequential processes differ from those previously found for sequential dissociation [15] in two respects: First, in multisequential

dissociation the E_{KER} is higher due to the higher excitation energy. Second, if any radiative cooling occurs before the first decay in the sequential process it will be strongly reduced in the multisequential decay, since, presumably, the evaporative rate constant increases much stronger with excitation energy than the radiation [10]. Conversely, if the radiation can be ignored in the calculation of the dissociation energy, the data can be used to test whether the kinetic-energy releases can be calculated from equilibrium properties, or, in other words, give an upper limit on the equilibration time of the photoexcitation. These considerations will be made quantitative in the results and discussion section below.

III. EXPERIMENTAL SETUP AND PROCEDURE

The experimental setup has already been described in detail elsewhere [15,22–24] and is identical to that used in [15,26]. Briefly, the cluster ions are produced in a Smalley-type laser vaporization source and transferred to the Penning trap, where they are size selected by resonant ejection of all other clusters. The ion ensemble is then centered radially and thermalized to the trap temperature of about 300 K with an argon gas pulse. The clusters are photoexcited by multiple photon absorption in a single pulse of a Nd:YAG-pumped dye laser with photon energies from 2 eV to 6 eV (YAG is yttrium aluminum garnet). After a variable delay period typically between 10 μs and 60 ms, the precursor and fragment abundances are measured in a time-of-flight mass spectrometer. By variation of the storage period between photoexcitation and ejection it is possible to monitor the delayed time-resolved dissociation process [25]. All steps of the multisequential and sequential dissociation before the last decay occur very fast compared to the time scale of the last dissociation. Therefore, the duration of the first dissociation steps has no influence on the determination of the dissociation rate constant in the last step of the sequence.

The excitation energies are adjusted so that the delayed dissociation is observed to be time resolved with decay times of the order of several milliseconds. The Au_n^+ clusters of interest are known to decay exclusively by monomer evaporation for the relatively low energies, where the process can be measured time resolved [27,28]. This can be expected to hold also for higher excitation energies since a hypothetical dimer evaporation would imply that a very large energy would not be accounted for and, furthermore, that this energy matches precisely the previously determined dissociation energy. Also, all previously measured dimer-to-monomer branching ratios for gold cluster cations decrease with excitation energy [26].

As an example, Fig. 1 shows the fragment yields as a function of delay period for the multisequential fragmentation of Au_{18}^+. As can be seen from the relative intensities, about 10% of the Au_{18}^+-clusters have absorbed one or more photons and undergo fragmentation within 60 ms. About 8% have absorbed one photon and evaporate a neutral monomer with a rate constant of $(40\pm16)\ s^{-1}$. About 1.6% have absorbed two photons and sequentially evaporate two monomers, the last of which is evaporated and delayed at a rate constant of $(44\pm18)\ s^{-1}$. Finally, about 0.4% have absorbed three photons and sequentially evaporate three monomers, the last of which is evaporated delayed at a rate constant of $(217\pm44)\ s^{-1}$. In measurements similar to that shown in Fig. 1, the build up rate constant of the third fragment (Au_{15}^+ in Fig. 1) has been determined for several initial excitation energies to cover the whole range of rate constants observable within the experimental time window.

The number of absorbed photons that induce a certain reaction can, in principle, be assigned unambiguously only in terms of differences. In general there is no way of knowing with certainty the absolute number of photons absorbed in a given decay chain. But if the *difference* in the number of photons were assigned incorrectly, the rate constants as a function of energy for the two different decay chains would have different slopes for the same rate constants. Hence, the procedure comes equipped with a clear experimental consistency check. For the decays involved in this work we can even assign absolute numbers to each chain with high plausibility since the fragmentation behavior of the clusters under investigation is well known from previous experiments [15,26].

IV. ANALYSIS AND RESULTS

A. Dissociation energies

First, the dissociation energies will be extracted from the data under the assumption that radiative cooling during the first evaporation steps can be ignored. This assumption will be treated in the following section.

Figure 2 shows the decay rates as a function of photoexcitation energy for the last step of the multisequential process $Au_{18}^+ \rightarrow Au_{17}^+ \rightarrow Au_{16}^+ \rightarrow Au_{15}^+$ (triangles) and the sequential process $Au_{17}^+ \rightarrow Au_{16}^+ \rightarrow Au_{15}^+$ (circles) (Fig. 2, top). Also shown (Fig. 2, bottom) are the decay constants for the last step of the sequential decay $Au_{18}^+ \rightarrow Au_{17}^+ \rightarrow Au_{16}^+$ (circles) and the direct decay $Au_{17}^+ \rightarrow Au_{16}^+$ (squares).

The shift in photoexcitation energy between multisequential and sequential rate constants (and likewise between sequential and direct rate constants) is determined as follows: The two datasets are simultaneously fitted with a smooth function of the form

$$ln\,(k) = ln(k_0) + aE + bE^2,$$
$$ln\,(k) = ln(k_0) + a(E - \Delta E_0) + b(E - \Delta E_0)^2, \tag{6}$$

where ΔE_0 is the energetic shift between the datasets. The points are weighted according to the relative uncertainty $\sigma(k_i)$ of the rate constants k_i with the factor $g_i = \sigma^{-2}(k_i)/\Sigma_l \sigma^{-2}(k_l)$ for the point *i*. From the energetic deviations, Δe_i, of the individual data points from the fitted curve, the uncertainties $\sigma(E_0)$ of E_0 and $\sigma(E_0 + \Delta E_0)$ of $E_0 + \Delta E_0$ are determined. The uncertainty of the position of one of the two curves is estimated as the root mean square of the deviations Δe_i of the measured rate constants from the fitted curve with a new set of weight factors g_i. With n data points for the curve and n_f fit parameters, only the $n - n_f$ points with the largest deviations are included in the error

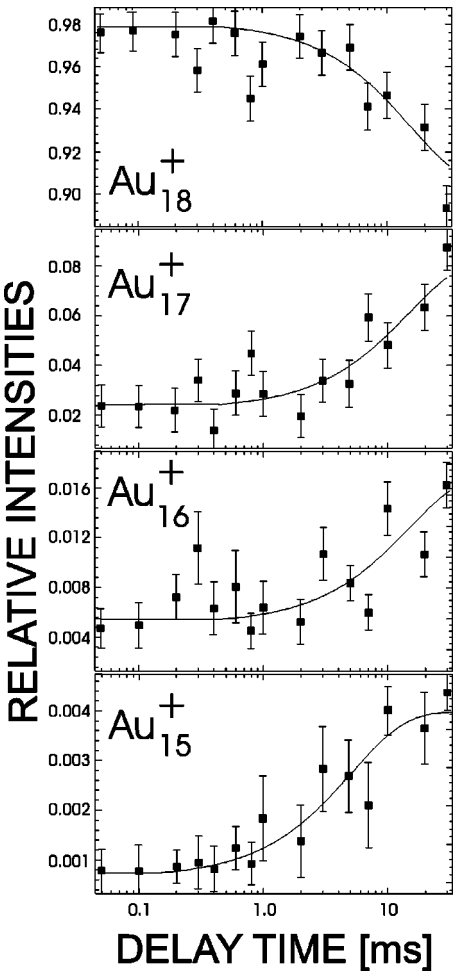

FIG. 1. Relative cluster intensities as a function of the delay period between photoexcitation and detection. Example of the sequential decay $Au_{18}^{+} \rightarrow Au_{17}^{+} \rightarrow Au_{16}^{+} \rightarrow Au_{15}^{+}$ after excitation with a 10-ns laser pulse at 3.99 eV photon energy and a pulse energy of 200 μJ. The lines are exponential curves fitted to the data.

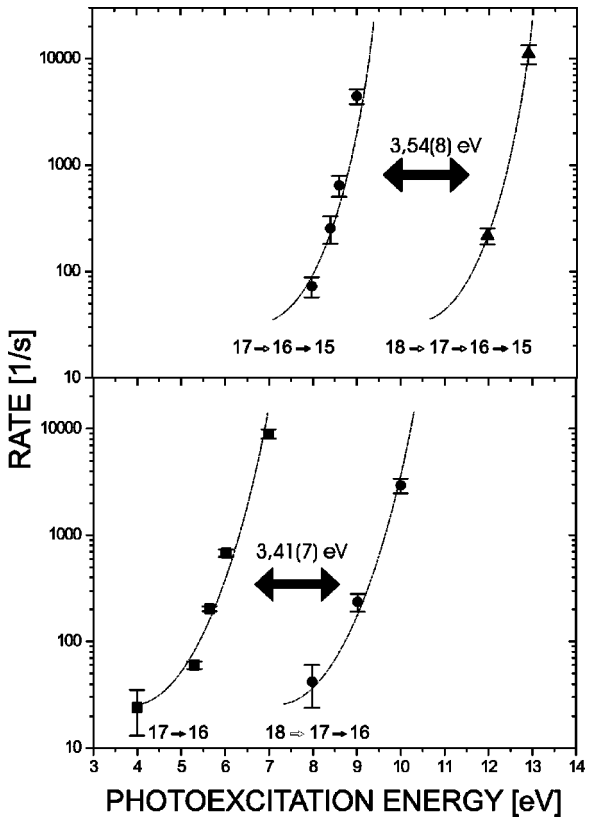

FIG. 2. Evaporative rate constants as a function of the excitation energy in sequential (circles) and multisequential dissociation processes (triangles), which lead to Au_{15}^{+} as the final state (top) and the corresponding direct (squares) and sequential dissociation rate constants (circles) with Au_{16}^{+} as the final state (bottom).

calculation, and the weights are recalculated including these points only. The average is multiplied by the factor $\sqrt{\Sigma_l g_l^2}$, which accounts for the effective number of points on the curve. Since in all cases, more decay rates corresponding to the curve for the sequential rate constants than to the curve for the multisequential rate constants have been measured, these rate constants determine the shape of the curve (6) predominantly. Therefore, $n_f=3$ fit parameters are assigned to the curve fitted to the sequential-decay data and the remaining parameter for the shift ΔE_0 is assigned to the curve fitted for the multisequential-decay data [29]. The square of the uncertainty of the energetic shift between the curves $\sigma(\Delta E_0)$ is then given by adding the squares of $\sigma(E_0)$ and $\sigma(E_0+\Delta E_0)$.

The only term in Eq. (3) not specified so far is the kinetic-energy release E_{KER}, which is a function of the microcanonical temperature $T(E_{ph}(n,n-3)-D_n+E_{th,n})$ of the $(n-1)$ product cluster. The functional dependence is calculated using detailed balance with due consideration of the influence of the attractive r^{-4} polarization potential between the cluster and the atom [18,10]. The kinetic-energy is distributed according to $p(\epsilon)d\epsilon \propto \epsilon\sigma(\epsilon)e^{-\epsilon/k_BT}d\epsilon$, where σ is the capture cross section and T is the microcanonical temperature of the cluster after dissociation. It is calculated classically and is a combination of the Langevin cross section at low energies and a geometric cross section modified by a polarization dependent term at high energies; $\sigma=\pi r_0^2(1-V_0/\epsilon)$, where $V_0 \equiv -e^2\alpha/4\pi\epsilon_0 2r_0^4$ is the polarization potential at the contact distance r_0 and α is the gold atom polarizability [30]. For r_0 we use the value $r_0=r_s[1+(n-1)^{1/3}]$ (r_s is the Wigner-Seitz radius [31]). The E_{KER}, which is the average of ϵ, is calculated numerically in terms of the scaled variable $p=|V_0/k_BT|$. A convenient (and material independent) approximate formula is given by

$$E_{KER}=k_BT[\tfrac{3}{2}+\tfrac{1}{2}\exp(a_1p+a_2p^2+a_3p^3)], \qquad (7)$$

with parameters $a_1=-1.892$, $a_2=0.311$, and $a_3=-0.054$. At low temperatures atoms are emitted with a distribution proportional to $\epsilon^{1/2}$, corresponding to the Langevin cross section, and consequently $E_{KER}=3/2k_BT$. At high temperatures where polarization forces become irrelevant, the result is geometric, $E_{KER}=2k_BT$, and Eq. (7) expresses the interpolation between these two limits.

Harmonic-oscillator heat capacities are used to calculate the cluster temperatures after dissociation, with the correction of $1k_B$ found in [33]. The gold bulk heat capacities per

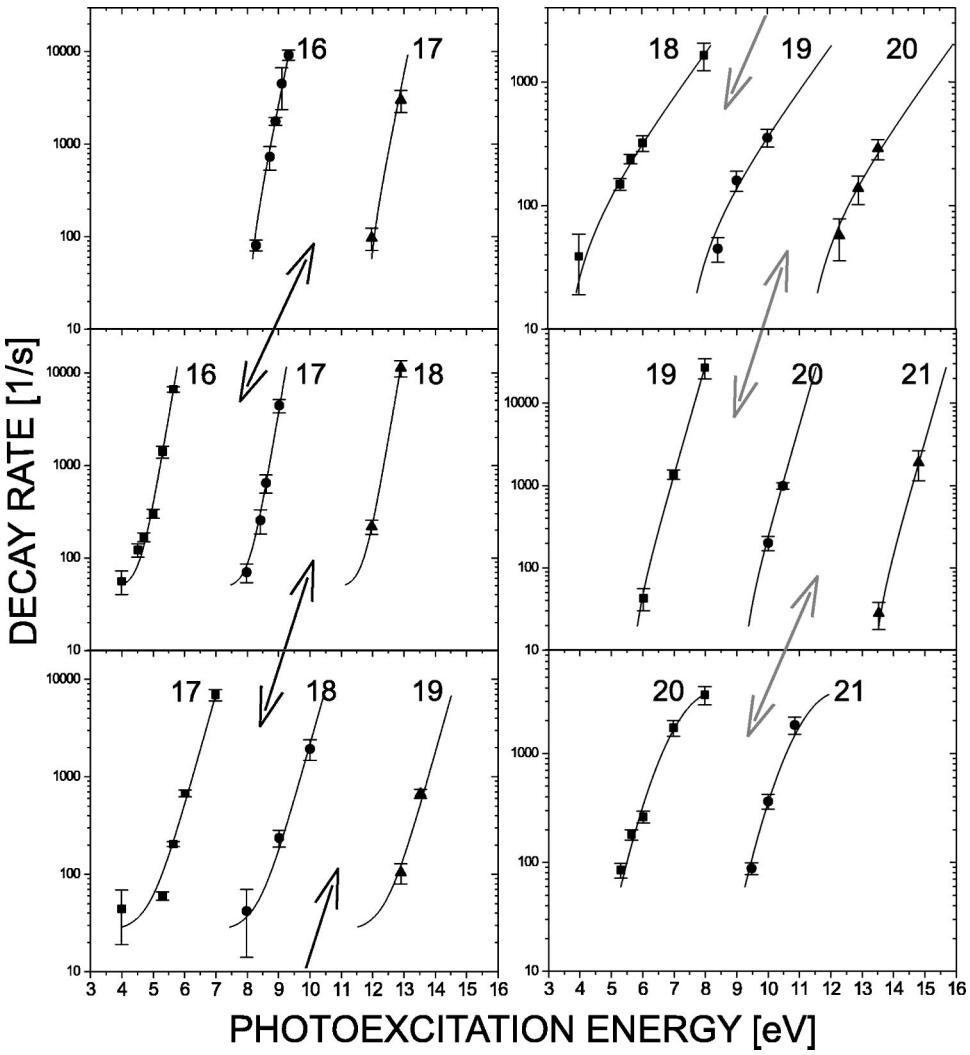

FIG. 3. Evaporative rate constants as a function of the photoexcitation energy for direct (squares), sequential (circles), and multisequential (triangles) dissociation processes. The numbers indicate the cluster size of the photoexcited precursor ion.

atom are close enough to this value to justify the choice. Melting does not seem to play an important role in this context, as judged by theoretical results which suggest that the latent heat of the small cluster sizes investigated here is consistent with zero [32].

Thus, the cluster temperature after dissociation is given by

$$T_{n-1}(n,n-i)=300\ \mathrm{K}+\frac{1}{k_B}\frac{E_{ph}(n,n-i)-D_n}{3(n-1)-7},\quad i=2,3. \tag{8}$$

Both the kinetic-energy release and the dissociation energies can be determined with Eqs. (3), (7), and (8).

Figure 3 gives a summary of all experimental results in terms of the decay constants as a function of the photoexcitation energies for the corresponding direct, sequential, and multisequential decays.

The values obtained for the monomer dissociation energies of Au_n^+ ($n=17$–21) are given in Table I and shown in Fig. 4 together with the results from [15]. Table I also gives the combined values from both the measurements. The results from [15] have been reanalyzed together with the data

TABLE I. Comparison of the dissociation energies of Au_n^+ ($n=17$–21) from this work, from [15], and the combined results. The uncertainties include an estimated 10% systematic uncertainty on the kinetic-energy release.

	Values from this work			Values from Ref. [15]			
n	ΔE_0 (eV)	E_{KER} (eV)	D(eV)	ΔE_0 (eV)	E_{KER} (eV)	D(eV)	$\overline{D}$ combined
17	3.70(7)	0.38(4)	3.38(8)	3.47(6)	0.16(2)	3.36(6)	3.37(5)
18	3.54(8)	0.32(3)	3.28(9)	3.41(6)	0.17(2)	3.30(6)	3.29(5)
19	4.10(8)	0.33(3)	3.83(9)	3.95(7)	0.22(2)	3.79(7)	3.81(6)
20	3.85(7)	0.34(3)	3.57(8)	3.62(8)	0.19(2)	3.49(8)	3.53(6)
21	4.15(8)	0.31(3)	3.90(9)	3.99(6)	0.24(2)	3.81(6)	3.86(5)

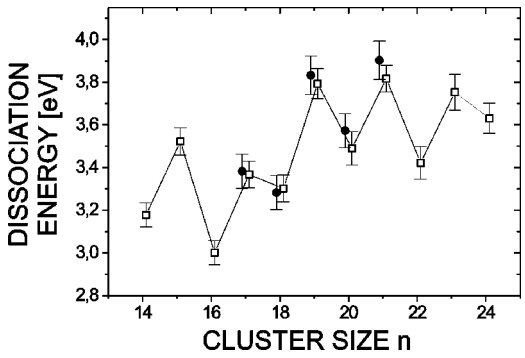

FIG. 4. Dissociation energies as a function of cluster size. Full symbols represent values obtained in multisequential dissociations (this work). Open squares correspond to values obtained in sequential dissociations [15]. The error bars include the estimated systematic uncertainties.

from the multisequential decays. The earlier analysis used a more conservative estimate of the uncertainties. The values of the dissociation energies are not affected.

B. Radiative cooling and kinetic-energy releases

As mentioned above, information about radiative cooling and the kinetic energy release can be extracted from the data. In the example of $n=18$ (Fig. 2) the energetic shift between the sequential (2) and the multisequential (1) processes calculated as described above is 3.54(8) eV, as compared to 3.41(7) eV for the shift between the direct and the sequential processes (5) and (4). The analogous results for the other processes measured, with different starting sizes *n*, show a similar higher shift for the chains involving more decays compared to the processes with fewer decays. This effect is readily understood with reference to Eqs. (3), (7), and (8) in terms of the increased kinetic-energy release for multisequential processes. The only E_{KER} that has an effect on the observed shifts is that of the first decay, both for the shift between the chains (1) and (2) and those involving the reactions (4) and (5). Since the longer chain requires more energy, by about one dissociation energy, the E_{KER} will consequently be higher. An order-of-magnitude estimate of the typical value of the difference in the kinetic-energy release for the two sets of processes is given by the difference in initial energy, about one dissociation energy, divided by the heat capacity of the product clusters, and multiplied with a numerical factor between 3/2 and 2 [see Eq. (7)]. This gives values for $E_{KER,n}(n,n-3)-E_{KER,n}(n,n-2)$ of the order of 0.15 eV.

Radiative energy loss has not been considered so far. If it is included, the energy of the cluster in the last, time-resolved, evaporation step of the multisequential reaction (1) is given by

$$E_{n-2}(n,n-3)=E_{th,n}+E_{ph}(n,n-3)-E_{KER,n-1}(n,n-3)-E_{KER,n}(n,n-3)-E_{rad,n}(n,n-3)-E_{rad,n-1}(n,n-3)-D_n-D_{n-1}, \quad (9)$$

where the new term, the radiative cooling $E_{rad,n}(n,n-3)$ is the total energy lost due to radiation by Au_n^+. It is the product of the radiated power $P_n(n,n-3)$ and the evaporative lifetime of the cluster, and is a stochastic quantity similar to the kinetic-energy release. For simplicity, radiative cooling is treated by use of the average value, i.e., $E_{rad,n}(n,n-3)=P_n(n,n-3)/k_n(n,n-3)$.

For the sequential reaction (2) starting at cluster size $n-1$ the corresponding energy is

$$E_{n-2}(n-1,n-3)=E_{th,n-1}+E_{ph}(n-1,n-3)-E_{KER,n-1}(n-1,n-3)-E_{rad,n-1}(n-1,n-3)-D_{n-1}. \quad (10)$$

When the photon energies are adjusted such that the rate constants are equal, these two energies are identical, $E_{n-2}(n,n-3)=E_{n-2}(n-1,n-3)$. Thus, the kinetic-energy release and the radiative cooling is the same for the last step and hence

$$D_n=E_{ph}(n,n-3)-E_{ph}(n-1,n-3)+E_{th,n}-E_{th,n-1}-E_{KER,n}(n,n-3)-E_{rad,n}(n,n-3). \quad (11)$$

A similar calculation for reactions (4) and (5), which stop one cluster size higher, gives

$$D_n=E_{ph}(n,n-2)-E_{ph}(n-1,n-2)+E_{th,n}-E_{th,n-1}-E_{KER,n}(n,n-2)-E_{rad,n}(n,n-2). \quad (12)$$

These equations show explicitly that only the kinetic-energy release in the first decay and the radiative cooling of the initial cluster have any influence on the value determined for the dissociation energy. Subtracting the two equations (11) and (12) gives the relation

$$[E_{ph}(n,n-3)-E_{ph}(n-1,n-3)]-[E_{ph}(n,n-2)-E_{ph}(n-1,n-2)]=[E_{KER,n}(n,n-3)+E_{rad,n}(n,n-3)]-[E_{KER,n}(n,n-2)+E_{rad,n}(n,n-2)]. \quad (13)$$

Consequently, the sum of the kinetic-energy release and the radiative cooling is constrained by the photoexcitation energies.

The radiative energy loss in Eq. (13) occurs from the same cluster of size n, but at different energies. The high-energy process emits more radiative power but is active for a much shorter time, since the evaporation rate increases much more rapidly with energy than the radiative power. This means that $E_{rad,n}(n,n-3)\ll E_{rad,n}(n,n-2)$ and that a comparison of the left-hand side of Eq. (13) with the right-hand side will show directly whether any energy is lost due to radiation of the initial cluster.

A potential systematic uncertainty in the E_{KER} should be pointed out. The rate constants may be high enough to induce decay before the last photon is absorbed. This would lead to a smaller kinetic-energy release than calculated here, a reduction of typically 0.15 eV as calculated above and can,

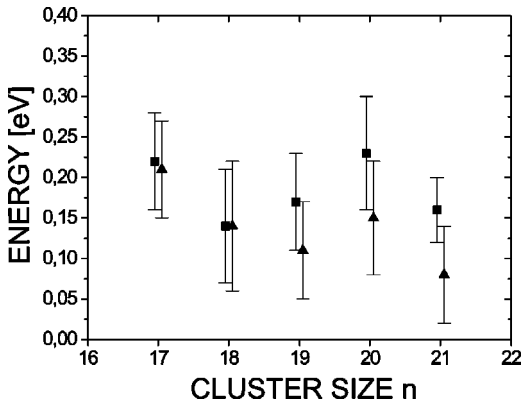

FIG. 5. Left hand side of Eq. (13) (squares) and $E_{KER,n}(n,n-3)-E_{KER,n}(n,n-2)$ (triangles) as a function of cluster size. The error bars on the kinetic-energy release difference represent the estimated systematic value, while those of the photoexcitation energies are derived from the measured shifts.

at the most, give a radiative cooling corresponding to the left-hand side of Eq. (13) (see Fig. 5). The problem only arises if the rate constant at the intermediate energies, around 10 eV, exceeds the reciprocal of the duration of the laser pulse, $k>10^8$ s^{-1}. It does not seem likely but in the absence of direct evidence we cannot conclusively rule it out.

Fig. 5 shows the experimental energy values of the left-hand side of Eq. (13) as a function of cluster size, and the right hand side values of Eq. (13) when the radiation energy loss is ignored. The kinetic-energy release is a small part of the shift ΔE_0 and the uncertainties in the difference of the shifts are correspondingly relatively large. The difference between the two energy values shown in Fig. 5, i.e., the energy lost due to radiation, does in no case exceed 0.08 eV with an uncertainty of about 0.1 eV and is thus consistent with zero.

The absence of radiative energy loss can be made plausible by a calculation of the time available for radiation before the first decay step. To this end, measured rate constants $k_n(E_{\mathrm{I}})$ in direct decays are extrapolated to decay rates $k_n(E_{\mathrm{II}})$ of the first step of the corresponding sequential decay initiated by the higher excitation energy $E_{\mathrm{II}}>E_{\mathrm{I}}$ by use of the relation

$$k_n(E_{\mathrm{II}})=k_n(E_{\mathrm{I}})\exp\left(\frac{D_n}{T'(E_{\mathrm{I}}-D_n/2)}-\frac{D_n}{T'(E_{\mathrm{II}}-D_n/2)}\right), \tag{14}$$

where T' is the effective emission temperature given by [33]

$$T'(E)=300\ \mathrm{K}+\frac{1}{k_B}\frac{E}{3n-7}. \tag{15}$$

The reliability of this extrapolation is limited, but it will be sufficient to demonstrate the point. The photoexcitation energy for the low-energy reference rate constant E_{I} is chosen so that $k_{n-2}(E_{\mathrm{I}})=1000$ s^{-1} and is found from the curves for the direct decay, $\mathrm{Au}_{n-2}{}^+\rightarrow\mathrm{Au}_{n-3}{}^+$. The value of E_{II} is chosen from the sequential and multisequential curves as the energy where the rate constant of the final step is also 1000 s^{-1}. The precise choice is arbitrary but this value falls in the measured range. With this procedure the experimentally inaccesible rate constant for $n=17$ in the sequential decay $\mathrm{Au}_{17}{}^+\rightarrow\mathrm{Au}_{16}^+\rightarrow\mathrm{Au}_{15}{}^+$ is calculated to 2×10^6 s^{-1}. This means that the radiative power has to exceed 2×10^5 eV/s to produce an observable energy loss of even the small amount 0.1 eV, or, in other words, that the measurements are not sensitive to radiated powers less than about 10^5 eV/s. For the precursor in the multisequential decay chain, the limits are even higher. If such a high radiated power is scaled to the energy of the precursor in the direct decay with the estimate that it scales with T^6 [34], the energy lost before evaporation is about half the total excitation energy. The decay would therefore be completely quenched. This scenario is ruled out by the fact that the decay is actually observable.

Furthermore, independent of the above estimates, according to the results shown in Fig. 5 any radiative cooling would have to be compensated by an equal amount of excess kinetic-energy release. This would imply that the photoexcitation energy of the cluster has not equilibrated on the time scale of the first decay of the multisequential chain. For $n=18$ the rate constant can be be estimated as above and it gives an equilibration time exceeding 50 ns. Such long equilibration times seem quite unrealistic.

The conclusion is therefore that the data are consistent with no substantial radiative cooling and that the kinetic-energy releases can be calculated to a sufficient precision by the formulas given. While radiative cooling does not influence the model-free determination of binding energies, it may, on the other hand, explain the unexpected behavior of the evaporation rates reported in [15].

V. DISCUSSION

The results on the dissociation energies of cationic gold clusters may be put into perspective by comparison with the values of ionization potentials and electron affinities of previous investigations. The ionization potentials (IP) are available from electron impact ionization threshold measurements [35]. Experimental electron affinities (EA) can be found in [36]. These data are shown in Fig. 6 together with the present data for the dissociation energies $\mathrm{Au}_n{}^+$, $n=17$–21 (see averaged values in Table I) and the data for $\mathrm{Au}_n{}^+$, $n=14$–16, 14–24 from [26,15].

The dissociation energies show an odd-even alternation all the way from $n=14$ to $n=24$, the largest size under consideration. Odd-size cluster cations, i.e., those clusters with an even number of atomic valence electrons, are more stable than their even-size neighbors. This behavior is in agreement with the expectations from the jellium model [37], where mainly the number of valence electrons counts for the stability relative to the neighboring sizes. In this description the extent of the odd-even staggering may be taken as an indication for the amount of splitting of the levels in the mean-field potential of the cluster; the typical distance between two adjacent single particle levels, δE at the Fermi level is $\delta E=D_{n-1}+D_{n+1}-2D_n$. The expected value is, for a Fermi gas without any level bunching, $\delta E=4E_F/3n$. With

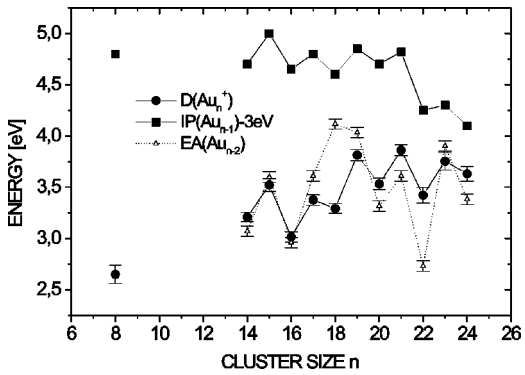

FIG. 6. Comparison of ionization potentials from [35] (full squares), electron affinities from [36] (open triangles), and average dissociation energy values from this work and from [15,26]. Note, that the IPs are shifted by one cluster size and the EAs by two cluster sizes to be isoelectric. Also, the IPs are lowered by 3 eV for visibility. For the IPs, no error bars are given in [35]. The EAs are considered to have an uncertainty of 0.05 eV [36].

the bulk Fermi energy, $E_F = 5.53$ eV, the ratio of observed to expected splitting is on the average 1.4. A value of unity suggests that the levels are evenly distributed according to the level distribution of a Fermi gas. The higher value observed indicates that the clusters are strongly deformed relative to a spherical mean-field potential.

The step in the dissociation energy between $n = 21$ and $n = 22$ is somewhat larger than most of the others and may indicate an electronic shell closing in terms of the jellium model [37]. However, its significance seems limited when compared with the step between $n = 14$ and $n = 15$ where no shell closing is expected.

The shell closing at $n = 21$ is more pronounced in the IP data, which qualitatively show the same odd-even effect. Note that in Fig. 6 the IP data points are shifted by one cluster size for an overlap of isoelectronic systems. Thus, $n = 21$ corresponds to 20 atomic valence electrons. The general trend of the IP is a decrease as a function of cluster size, whereas it is increasing for the dissociation energies. This behavior is expected from the liquid drop model when the charging energy is included. If one only focuses on the size-to-size variations, i.e., the magnitude of the odd-even oscillations, the two curves are seen to agree fairly well. The agreement for the EA values is not as obvious. However, with the exception of the point at $n = 16$ (note that the cluster sizes of the EA values are shifted by 2) the data follow the odd-even pattern as do the dissociation energies and IPs.

In principle, the measured ionization potentials V_n^{ion} allow a calculation of the neutral dissociation energies as

$$D_{n,0} = D_{n,+} + V_n^{\mathrm{ion}} - V_{n-1}^{\mathrm{ion}}. \tag{16}$$

This conversion unfortunately suffers from the combined uncertainties of the three terms on the right-hand side of the equation. Furthermore, the measured IPs are vertical, and in order to apply Eq. (16) the adiabatic values are needed. If nevertheless this formula is applied, the calculated values range from 3.2 eV to 3.7 eV, which is the same range as for the cations.

One reason for the attempted conversion of the available experimental dissociation energies for cations to values for neutrals is the fact that theoretical structures are calculated almost exclusively for the neutrals. The only calculated dissociation energy for a gold cluster cation is, to our knowledge, that for $n = 8$ found in [38], which has the value 2.01 eV (or 1.94 eV for a low-lying isomer). The calculations were done using the density-functional theory with a generalized gradient approximation functional and should be able to capture both odd-even and shell structure effects. However, the result falls short of the experimental value of 2.65 eV $\pm$ 0.09 eV [39] by a significant amount.

Given the similarity between the IPs and the dissociation energies, in the following the *D*'s for the charged species are identified with the isoelectronic neutral values. Wang *et al.* [40] have calculated the total ground-state energies for Au_n, $n = 2$–20, with an LDA algorithm. The results reproduce the odd-even variations in the $\Delta_2 E_n$ (E_n is the total ground-state energy of the *n*-atomic cluster) with a single exception ($n = 16$), but have a less pronounced structure in the neutral dissociation energy. If Eq. (16) is used with the calculated IPs from the same paper the odd-even variations are still deficient but the overall agreement is better, with the worst deviations of about 0.5 eV in two cases ($n = 15,20$). The geometries of the neutral and the charged species are close [41], so the differences in adiabatic and vertical ionization potentials are expected to be relatively small. An additional uncertainty is caused by the finite precision with which the data are given by the authors.

Wilson and Johnston have calculated the structures and energies of the sizes between $n = 2$ and $n = 40$ (neutrals only) with an empirical potential [42]. The potential contained parameters that were fitted to reproduce bulk properties and included three-body interactions. The geometrical structure of the clusters was then optimized with this potential. This type of calculation is not expected to reproduce the specific quantum-mechanical features. Indeed, the calculated neutral dissociation energies show no odd-even effect. In addition, they are on the average 0.5 eV below the measured (cationic) values.

At present, the theoretical studies agree neither with each other nor do they seem to reproduce the details of the experimental results. Obviously, there is a need for refined calculations in order to fully understand the small gold clusters and their properties. In particular, we would like to take the opportunity to point out the difficulties in experiments with size-selected neutral clusters and suggest that more effort be devoted to the structure of charged species.

VI. CONCLUSIONS

The dissociation energies found by the use of multisequential dissociation of small gold clusters agree with the previously determined values by use of sequential dissociation [15]. For all cluster sizes investigated ($n = 17$–21), ra-

diative cooling and excess kinetic-energy release are constrained by the data to be identical. It is argued that both can be assumed to be negligible at the measurement accuracy of 1% to 2 % of the dissociation energy. The odd-even effects in the dissociation energies are in good agreement with previous IP measurements.

ACKNOWLEDGMENTS

This work was supported by the DFG, the EU networks ''EUROTRAPS'' and ''CLUSTER COOLING,'' the ''Fonds der Chemischen Industrie,'' and by the Academy of Finland under the Finnish Center of Excellence Program 2000–2005.

[1] L.S. Kassel, J. Phys. Chem. **32**, 225 (1928).
[2] O.K. Rice and H.C. Ramsperger, J. Am. Chem. Soc. **50**, 617 (1928).
[3] V. Weisskopf, Phys. Rev. **52**, 259 (1937).
[4] R.A. Marcus, J. Chem. Phys. **20**, 359 (1952).
[5] C.E. Klots, J. Phys. Chem. **75**, 1526 (1971).
[6] P.C. Engelking, J. Chem. Phys. **85**, 3103 (1986).
[7] G.F. Bertsch, N. Oberhofer, and S. Stringari, Z. Phys. D: At., Mol. Clusters **20**, 123 (1991).
[8] S. Frauendorf, Z. Phys. D: At., Mol. Clusters **35**, 191 (1995).
[9] P.A. Hervieux and D.H.E. Gross, Z. Phys. D: At., Mol. Clusters **33**, 295 (1995).
[10] K. Hansen, Philos. Mag. B **79**, 1413 (1999).
[11] C. Brechignac, Ph. Cahuzac, J. Leygnier, and J. Weiner, J. Chem. Phys. **90**, 1492 (1989).
[12] C.E. Klots, Z. Phys. D: At., Mol. Clusters **20**, 105 (1991), and references therein.
[13] J.B. Griffin and P.B. Armentrout, J. Chem. Phys. **106**, 4448 (1997).
[14] J.U. Andersen, *et al.*, Phys. Rev. Lett. **77**, 3991 (1996).
[15] M. Vogel, K. Hansen, A. Herlert, and L. Schweikhard, Phys. Rev. Lett. **87**, 013401 (2001).
[16] A.J. Stace and A.K. Shukla, Chem. Phys. Lett. **85**, 157 (1982).
[17] M. Lundquist, *et al.*, Phys. Rev. Lett. **75**, 1058 (1995), and references therein.
[18] K. Hansen and J. Falk, Z. Phys. D: At., Mol. Clusters **34**, 251 (1995).
[19] S. Matt, *et al.*, Chem. Phys. Lett. **303**, 379 (1999).
[20] P. Brockhaus, *et al.*, Phys. Rev. A **59**, 495 (1999).
[21] J. Laskin and C. Lifshitz, J. Mass Spectrom. **36**, 459 (2001).
[22] L. Schweikhard, *et al.*, Phys. Scr. **T59**, 236 (1995).
[23] L. Schweikhard, *et al.*, Eur. Phys. J. D **9**, 15 (1999).
[24] S. Becker, *et al.*, Rev. Sci. Instrum. **66**, 4902 (1995).
[25] C. Walther, *et al.*, Chem. Phys. Lett. **256**, 77 (1996); **262**, 668 (1996).
[26] M. Vogel, K. Hansen, A. Herlert, and L. Schweikhard, Chem. Phys. Lett. **346**, 117 (2001).
[27] U. Hild *et al.*, Phys. Rev. A **57**, 2786 (1998).
[28] M. Vogel, K. Hansen, A. Herlert, and L. Schweikhard, Eur. Phys. J. D **16**, 73 (2001).
[29] The procedure is not rigorous but handles the different statistical uncertainties in the rates in an effective way.
[30] *CRC Handbook of Chemistry and Physics*, 76th ed., edited by David R. Lide (CRC Press, Boca Raton, 1995).
[31] N. W. Ashcroft and N. D. Mermin, *Solid State Physics* (Saunders, Philadelphia, 1976).
[32] F. Ercolessi, W. Andreoni, and E. Tosatti, Phys. Rev. Lett. **66**, 911 (1991).
[33] J.U. Andersen, E. Bonderup, and K. Hansen, J. Chem. Phys. **114**, 6518 (2001).
[34] J.U. Andersen, E. Bonderup and K. Hansen, J. Phys. B **35**, R1 (2002).
[35] C. Jackschath, I. Rabin, and W. Schulze, Ber. Bunsenges. Phys. Chem. **86**, 1200 (1992).
[36] K.J. Taylor, C.L. Pettiette-Hall, O. Cheshnovsky, and R.E. Smalley, J. Chem. Phys. **96**, 3319 (1992).
[37] W. Ekardt, Phys. Rev. Lett. **52**, 1925 (1984).
[38] S. Gilb, P. Weis, F. Furche, R. Ahlrichs, and M.M. Kappes, J. Chem. Phys. **116**, 4094 (2002).
[39] M. Vogel, K. Hansen, A. Herlert, L. Schweikhard, and C. Walther, J. Chem. Phys. **116**, 9658 (2002).
[40] J. Wang, G. Wang, and J. Zhao, Phys. Rev. B. (to be published).
[41] J. Zhao (private communication).
[42] N.T. Wilson and R.L. Johnston, Eur. Phys. J. D **12**, 161 (2000).